ELSEVIER

Biochimica et Biophysica Acta 1373 (1998) 282–288

BIOCHIMICA ET BIOPHYSICA ACTA
BBA

Rapid report

A unifying T_m diagram for phosphatidylethanolamines with *sn*-1 C_{20} saturated and *sn*-2 C_{18} unsaturated acyl chains

C. Huang *, G. Wang, H. Lin, S. Li

Department of Biochemistry and Molecular Genetics, Health Sciences Center, University of Virginia, Box 440, Charlottesville, VA 22908, USA

Received 30 April 1998; accepted 6 May 1998

Abstract

We have determined calorimetrically the phase transition temperature (T_m) values of five *sn*-1 saturated/*sn*-2 unsaturated phosphatidylethanolamines (PE) in which the *sn*-1 acyl chain has 20 carbons and the *sn*-2 acyl chain has 18 carbons with different number and position of the *cis* double bond. When these T_m values are combined with the five published T_m values of related unsaturated PE, a unifying T_m diagram is generated for the first time. Moreover, as the molecular mechanics simulated structures of these lipids are taken into consideration, this unifying T_m diagram provides insight into how variations in the number and position of the *cis* double bond in the lipid's *sn*-2 acyl chain can influence the phase transition behavior of the lipid bilayer.

Keywords: Phase transition temperature; Differential scanning calorimetry; Molecular mechanics simulation

Diacyl phospholipids isolated from biological membranes are amphipathic molecules with distinct polar and non-polar moieties. As a result, they usually self-assemble in aqueous solution, at physiological temperatures, to form large aggregates called the lipid bilayers. Interestingly, one-component phospholipids constituting the bilayers in the aqueous dispersion may, upon heating, exhibit multiple phase transitions. Of the several transitions, the main phase transition or the gel-to-liquid crystalline phase transition is the only one that is observed reproducibly upon repeated reheatings. The characteristic temperature corresponding to the maximal peak height of the sharp main transition is denoted as the phase transition temperature or T_m which can be most accurately determined by high-resolution differential scanning calorimetry (DSC).

The thermally induced structural changes of the lipid bilayer accompanying the main phase transition at T_m have been studied extensively over the years, and the most fundamental process underlying these changes at T_m is the abrupt occurrence of the *trans* $\rightarrow$*gauche* rotational isomerizations of methylene groups in the lipid chains (for recent reviews, see [1–3]). Consequently, one can appreciate that the T_m value is related to, among other factors, the number of *trans* rotamers or *trans* C-C single bonds present in the lipid chains at $T < T_m$. A given lipid species within a subclass of diacyl phospholipid is specified by the chemical compositions of the fatty acids esterified at the *sn*-1 and *sn*-2 positions of the glycerol backbone, which, at $T < T_m$, must contain a

* Corresponding author. Fax: +1 (804) 9245069; E-mail: ch9t@virginia.edu

0005-2736/98/$19.00
PII: S0005-2736(98)00092-3

certain fixed number of total *trans* C-C single bonds. As a result, such a lipid species is expected to exhibit, in excess water, a unique T_m value. This expectation is indeed borne out by experimental results obtained calorimetrically with saturated phosphatidylcholine (PC) and phosphatidylethanolamine (PE) [4]. We can take the homologous series of saturated identical-chain PC from C(14):C(14)PC to C(20):C(20)PC with an incremental increase of one methylene unit per acyl chain as examples. In this series of lipids, not only each of the seven PC species has its own unique value of T_m, the T_m value is also observed to increase nearly linearly from 24.1°C for C(14):C(14)PC to 66.4°C for C(20):C(20)PC [4]. This increase in T_m with increasing carbon number in the lipid chains clearly demonstrates that T_m is closely related to the total number of *trans* C-C single bonds present in the lipid chains at $T < T_m$.

We have just seen that the experimental T_m value may be regarded as a unique physical constant for a given phospholipid species. Now, we shall see that T_m may be used further as a simple comparative means to yield information about the dynamic structure of unsaturated lipid molecules packed in the gel-state bilayer. This point can be simply illustrated by considering saturated C(16):C(16)PC and monounsaturated C(16):C(18:1Δ^9)PC. These two lipid species have the same total number of 28 methylene units in their respective acyl chains. In addition, C(16):C(16)PC, the best studied phospholipid [5], is well known to be highly ordered in the gel-state bilayer with both chains mostly in all-*trans* configurations. The T_m values of C(16):C(16)PC and C(16):C(18:1Δ^9)PC are 41.5°C and −2.6°C, respectively [3]. The significantly lower T_m value means that C(16):C(18:1Δ^9)PC, in comparison with C(16):C(16)PC, has a smaller number of *trans* C-C bonds and, concomitantly, a larger number of *gauche* C-C bonds in its acyl chains at $T < T_m$. Therefore, on the basis of T_m, C(16):C(18:1Δ^9)PC can be regarded as being partially disordered in the gel-state bilayer. Furthermore, C(16):C(18:1Δ^9)PC differs from C(16):C(16)PC in the chemical composition of the *sn*-2 acyl chain. The partially disordered state of C(16):C(18:1Δ^9)PC at $T < T_m$ may thus be reasonably attributed to the effect of *sn*-2 acyl chain unsaturation; hence, the large population of *gauche* rotamers may be assigned to be in the *sn*-2 acyl chain. In the absence of supplementary data, this is as far as T_m alone can take us toward the elucidation of the dynamic structure of an unsaturated lipid in the gel-state bilayer.

The introduction of a single *cis* double bond (Δ) into the middle of a long *sn*-2 acyl chain of PC can be shown by molecular mechanics (MM) calculations to have two important consequences [6]. (1) The long *sn*-2 acyl chain is transformed into two shorter segments linked by a Δ-containing kink. This kinked *sn*-2 acyl chain has a crankshaft-like topology. (2) The two C-C single bonds adjacent to the rigid *cis* carbon-carbon double bond are highly flexible at $T < T_m$. Combining the structural and dynamic information obtained with MM calculations just cited and the experimental T_m values obtained with several homologous series of mixed-chain phospholipids with the *cis* double bond at different positions in the *sn*-2 acyl chain allows us to still farther specification of unsaturated lipid systems. In fact, based on the combined approach, a molecular model about the dynamic structure of unsaturated lipid in the gel-state bilayer is beginning to emerge [7,8]. In this communication, we have determined the T_m values of five *sn*-1 saturated/*sn*-2 unsaturated PE in which *sn*-1 and *sn*-2 acyl chains have 20 and 18 carbons, respectively. The numbers and positions of *cis* double bonds in the *sn*-2 acyl chain, however, vary from lipid to lipid. These calorimetrically determined T_m values and five previously published T_m values of the corresponding positional isomers, also from this laboratory, were codified. Based on this codification, a unifying T_m diagram is formed for the first time. The variations in T_m observed in this unifying T_m diagram can be interpreted by the MM-based molecular model.

Mixed-chain *sn*-1 saturated/*sn*-2 unsaturated PE was synthesized from the corresponding PC by the base-exchange reaction in the presence of excessive amounts of ethanolamine hydrochloride, at pH 5.6, using phospholipase D according to the method of Comfurius and Zwaal [9] as described in detail elsewhere [8,10]. The mixed-chain PC was semisynthesized using the established procedure reported previously [11]; however, the in situ reaction, and the reacylation were carried out strictly under N_2 to avoid possible lipid oxidation. All lipids were purified by column chromatography on silica gel 60 and

exhibited only one spot on thin-layer chromatography in $CHCl_3/CH_3OH/5\%$ NH_4OH (65:30:5). Saturated lysophosphatidylcholine with eicosanoyl chain, one of the starting materials for the semisynthesis of PC, was obtained from Avanti (Alabaster, AL). Unsaturated fatty acids, the other starting materials, were purchased from Sigma (St. Louis, MO) or Metreya (Pleasant Gap, PA); however, *cis*,*cis*-12,15 (or 6,9)-octadecadienoic acid was synthesized by the modified method of Christie and Holman [12].

The high-resolution DSC experiments were carried out using a MicroCal MC-2 calorimeter (Northampton, MA) or a Hart 7708 calorimeter (Pleasant Grove, UT). A constant scan rate of 15°C/h running in the ascending temperature mode was used. All reported DSC data were collected from the second DSC heating scan as described previously [8]. The T_m value obtained at the transition peak maximum from the second DSC heating run was reproducible at ± 0.1°C.

All MM force field calculations were carried out using an IBM RS/6000 computer workstation. The software MM3 (version 92) for MM calculations was supplied by Quantum Chemistry Program Exchange (Chemistry Department, Indiana University, Bloomington, IN). The structural data from the output of MM3 computations were transferred into the HyperChem 4.0 software (Hyper Cube, Waterloo, Canada) performed on a Pentium P5-200 platform, from which the graphic images of lipid molecules can be visualized. Details of the procedure for obtaining the energy-minimized structure for various *sn*-1 saturated/*sn*-2 unsaturated PE were described previously [6–8]. Briefly, prior to stochastic search for the energy-minimized conformation of *sn*-1 saturated/*sn*-2 unsaturated PE, the atomic coordinates of an initially approximate structure obtained from the single crystal structure of C(12):C(12)PE [13] and the energy-minimized unsaturated chain [14] were generated. Any additional methylene-interrupted *cis* double bonds for the *sn*-2 acyl chain were constructed using $s^-\Delta s^+s^+\Delta s^-$ (or $s^+\Delta s^-s^-\Delta s^+$) as the added sequence [14], where $s^{\pm}$ refers to *skew* ($\pm$) conformations with torsion angles of about ± 110° and Δ denotes *cis* double bond with torsion angle of about 0°. These initial coordinates of the crude structural model were used as a set of initial input data in MM calculations.

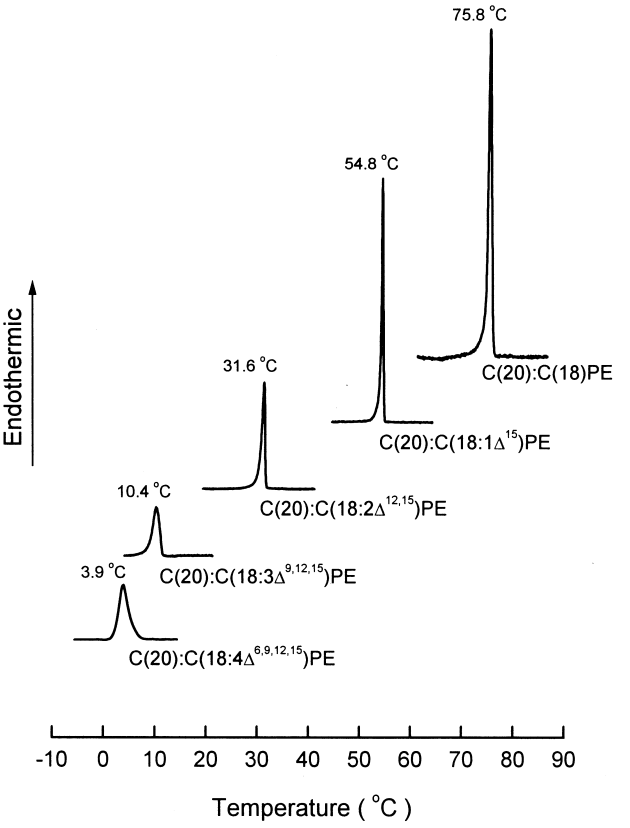

Fig. 1. A series of second DSC heating scans for aqueous dispersions of C(20):C(18)PE and its ω3 unsaturated derivatives. These DSC curves show a continuous decrease in T_m with a stepwise increase in the number of the *cis* double bond in the lipid's *sn*-2 acyl chain. Each T_m value is indicated above its associated main phase transition.

In Fig. 1 the second DSC heating curves for aqueous dispersions prepared individually from C(20):C(18)PE and its four unsaturated ω3 derivatives are illustrated. These unsaturated ω3 PE derivatives have one to four *cis* double bonds in their *sn*-2 acyl chains, and they are: C(20):C(18:1Δ^{15})PE, C(20):C(18:2$\Delta^{12,15}$)PE, C(20):C(18:3$\Delta^{9,12,15}$)PE, and C(20):C(18:4$\Delta^{6,9,12,15}$)PE. The aqueous dispersion prepared from saturated C(20):C(18)PE exhibits a sharp, single, and nearly symmetric endothermic transition with a T_m of 75.8°C. After the first *cis* double bond is introduced into C(20):C(18)PE at the third carbon (ω3) when counting from the methyl end of the *sn*-2 acyl chain, the resulting C(20):C(18:1Δ^{15})PE also exhibits a sharp, single and nearly symmetric phase transition curve. However, this transition is downshifted markedly by 21.0°C with a T_m of 54.8°C (Fig. 1). This large de-

crease in T_m cannot be explained simply by the decrease of one C-C single bond number in the *sn*-2 acyl chain as a result of the incorporation of a single *cis* double bond in between C(15) and C(16), since a considerably smaller difference of 3.9°C in T_m between C(20):C(18)PE and C(20):C(17)PE has been documented [4].

The observed large difference in T_m between monoenoic phospholipid and its saturated counterpart has been hypothesized as due to the presence of a partially disordered short segment in the monoenoic *sn*-2 acyl chain at $T < T_m$ [7,8]. This disordered segment does not contribute significantly to the chain melting process of *trans*→*gauche* isomerizations at T_m. In the case of C(20):C(18:1Δ^{15})PE, the disordered segment is the terminal segment of -C(15) = C(16)-C(17)-C(18). The assumed flexible nature of this terminal segment at $T < T_m$ can be attributed mainly to the large degrees of rotational freedom of the two single C-C single bonds adjacent to the *cis* double bond as demonstrated by MM calculations [6]. Data in strong support of the proposed model comes from the T_m of C(20):C(14)PE, which is 54.6°C [4], and is virtually identical to the T_m of 54.8°C observed for C(20):C(18:1Δ^{15})PE as shown in Fig. 1. Fig. 1 further shows that the phase transition temperatures of other ω3 unsaturated derivatives of C(20):C(18)PE downshift progressively as additional *cis* double bonds are incorporated successively into the *sn*-2 acyl chain.

The molecular structures of these ω3 PEs can be simulated by MM calculations and they are illustrated in Fig. 2. Each energy-minimized ω3 lipid is characterized by a kinked *sn*-2 acyl chain in which two segments are linked by a Δ-containing kink sequence. The upper segment extends from the C(3) carbon to the olefinic carbon with the lowest number. The all-*trans* segment designated by ATS is one C-C bond length less than the upper segment, because the C-C single bond preceding the *cis* double bond has a *skew* (+) conformation with a torsion angle of about 110°. One can easily recognize from various ω3 lipids shown in Fig. 2 that the all-*trans* linear segment in the unsaturated *sn*-2 acyl chain becomes progressively shortened as methylene-interrupted *cis* double bonds are stepwise incorporated into the chain on the carboxyl side of the existing double bond. This progressively shortened

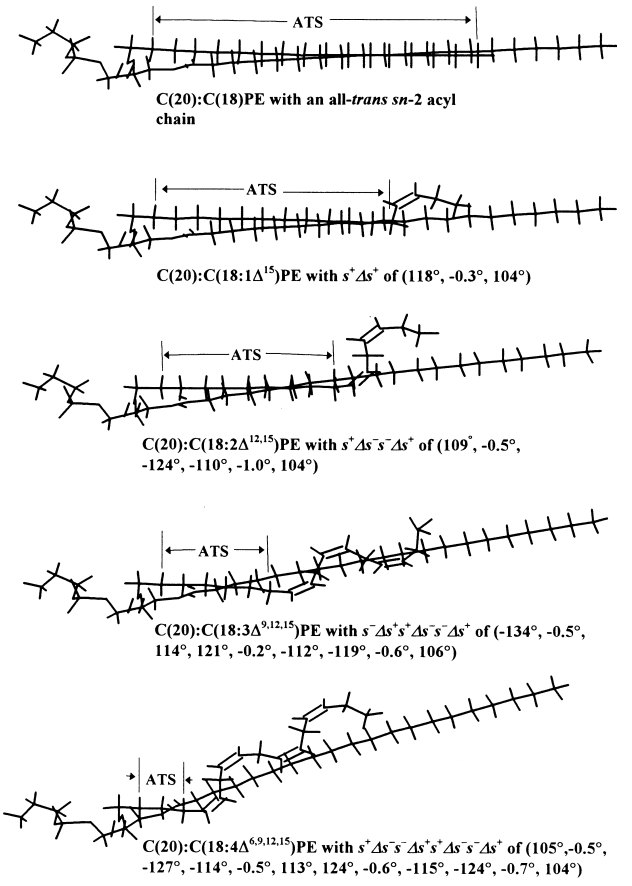

Fig. 2. Molecular graphics representations of the energy-minimized structures of C(20):C(18)PE and its ω3 unsaturated derivatives. The all-*trans* segment (ATS) in each kinked *sn*-2 acyl chain is indicated, and it decreases with increasing number of the *cis* double bond.

ATS at $T < T_m$ can thus account for the observed successive decrease in T_m for ω3 PE as depicted in Fig. 1.

Similar to ω3 PE, the T_m values of ω6 PE and ω9 PE, relative to that of C(20):C(18)PE, are also observed to decrease significantly with the incorporation of the first *cis* double bond. Subsequent incorporation of additional *cis* double bonds on the carboxyl side of the existing double bond further reduces the T_m and the results are given in the middle two rows in the T_m diagram shown in Fig. 3. Together with ω3 PE, these data indicate clearly that the T_m value associated with the gel-to-liquid crystalline phase transition of the lipid bilayer composed of *sn*-1 saturated/*sn*-2 ω unsaturated PE is strongly influenced by the number of *cis* double bonds present in the lipid's *sn*-2 acyl chain.

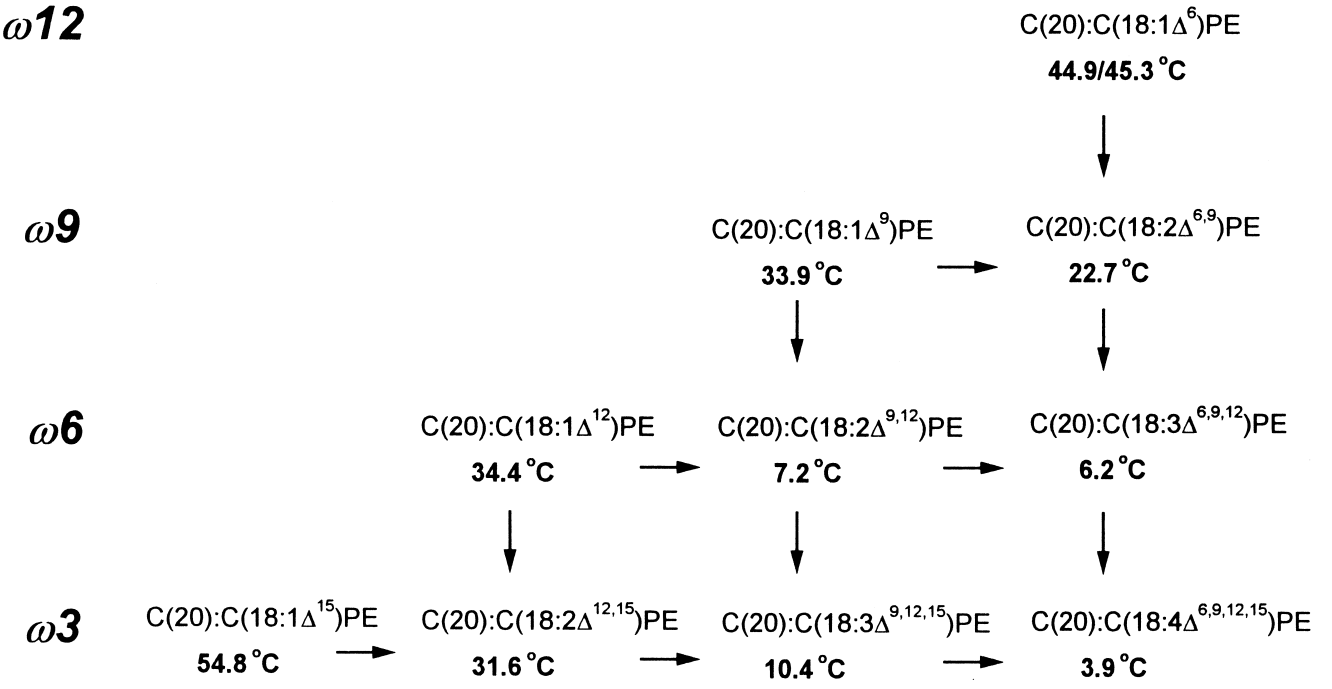

Fig. 3. A unifying T_m diagram for unsaturated lipids derived from a common precursor, the C(20):C(18)PE. Each row is specified by a family of omega lipid(s) as indicated. The T_m values are printed in bold face under their corresponding lipids. Five T_m values are obtained calorimetrically from the present investigation and they are associated with the following lipids: C(20):C(18:1Δ^6)PE, C(20):C(18:1Δ^{15})PE, C(20):C(18:2$\Delta^{6,9}$)PE, C(20):C(18:2$\Delta^{12,15}$)PE, and C(20):C(18:3$\Delta^{6,9,12}$)PE. The other five T_m values are taken from the literature [7,8], also published from this laboratory.

The T_m values of various C(20):C(18)PE derivatives shown in the T_m diagram (Fig. 3) can also be viewed along the vertical column from top to bottom. Unlike those lipid species shown horizontally, these unsaturated lipids have their *cis* double bonds added successively on the methyl side of the existing double bond. Let us first look at the last column which contains the largest number of lipid species. The first *cis* double bond is incorporated at the Δ^6 position near the carboxyl end. The resulting C(20):C(18:1Δ^6)PE, in excess water, exhibits calorimetrically a sharp yet split peak. Hence, two T_m values of 44.9°C and 45.3°C are given in Fig. 3. All other unsaturated PEs display calorimetrically a single gel-to-liquid crystalline phase transition. The T_m associated with the single phase transition decreases with increasing number of the *cis* double bond (Fig. 3, last column). This T_m-lowering trend of successive chain unsaturation is analogous to that observed earlier for the series of ω3 PE shown in Fig. 1; hence, this characteristic trend can be explained by the gradual shortening of the all-*trans* segment in the *sn*-2 acyl chain due to the replacement of the C-C single bond by the C-C double bond.

Now let us see how the T_m varies for the series of unsaturated PE shown in the second column from the right in Fig. 3. The addition of the first *cis* double bond at the Δ^9 position near the middle of the *sn*-2 acyl chain in C(20):C(18)PE results in a large decrease in T_m from 75.8°C to 33.9°C. The addition of a second *cis* double bond at the Δ^{12} position results in a further decrease of 26.7°C in T_m as expected [8]. Interestingly, the addition of a third *cis* double bond at the Δ^{15} position is accompanied by a small *increase* of 3.2°C in T_m. This down-and-up trend in T_m has been observed previously for several series of unsaturated PEs from this laboratory [8]. Moreover, similar down-and-up trends in T_m have also been observed for two series of unsaturated PCs [15,16]. It should be emphasized, however, that in the present study the down-and-up trend in T_m is not presented as an isolated single series of lipids; instead, it is presented in a unifying diagram (Fig. 3) among all other related unsaturated PEs with differ-

ent number and position of the *cis* double bond and, furthermore, all these unsaturated PEs are derived from a common precursor, the C(20):C(18)PE.

The small increase in T_m accompanying the C(20):C(18:2$\Delta^{9,12}$)PE → C(20):C(18:3$\Delta^{9,12,15}$)PE conversion is intriguing, since the incorporation of a third *cis* double bond into the *sn*-2 dienoyl chain usually results in a decrease in T_m as seen in the following conversions (Fig. 3): C(20):C(18:2$\Delta^{6,9}$)PE or C(20):C(18:2$\Delta^{9,12}$)PE → C(20):C(18:3$\Delta^{6,9,12}$)PE and C(20):C(18:2$\Delta^{12,15}$) PE → C(20):C(18:3$\Delta^{9,12,15}$) PE. The difference between these two types of conversions lies in the position of the newly added *cis* double bond. In the first type, the newly added *cis* double bond occurs in the long segment of the kinked *sn*-2 dienoyl chain; hence, the total number of all-*trans* C-C single bonds in the resulting *sn*-2 trienoyl chain is reduced, leading to a decrease in T_m. The other type as exemplified by the C(20) : C (18:2$\Delta^{9,12}$) PE → C(20):C(18:3$\Delta^{9,12,15}$)PE conversion is characterized by the addition of a third *cis* double bond into the short lower segment of the *sn*-2 dienoyl chain. This short segment can be reasonably assumed to be disordered at $T < T_m$; hence, it does not contribute much to the chain melting process of *trans* → *gauche* isomerizations underlying the main phase transition at T_m. When a third *cis* double bond is introduced into this presumably disordered segment at the Δ^{15} position, the resulting trienoyl chain will remain largely in the same disordered state. The T_m of C(20):C(18:3$\Delta^{9,12,15}$)PE will, therefore, not decrease. Furthermore, due to the additional rotational immobility of the olefinic carbons about the newly added *cis* double bond, the configurational entropy of this trienoyl chain will decrease slightly at $T > T_m$ relative to its precursor, leading to a small increase in T_m.

The observed down-and-up trends in T_m suggests strongly that not only the number but also the position of the *cis* double bond in the *sn*-2 acyl chain can influence the main phase transition behavior of the lipid bilayer. The importance of the position of the *cis* double bond is, in fact, indicated by the diagonal terms presented in Fig. 3. For the series of monoenoic PE, it is clearly seen that the lipid with a *cis* double bond located nearly in the middle of the *sn*-2 acyl chain has the lowest value of T_m, a scenario well documented in the literature [7]. For the three dienoic PE species shown diagonally in Fig. 3, a similar but new profile is observed. In particular, C(20):C(18:2$\Delta^{9,12}$)PE with its two methylene-interrupted *cis* double bonds located nearly in the middle of the *sn*-2 acyl chain has the lowest T_m value. The virtue of the T_m diagram (Fig. 3) is that all different T_m profiles observed earlier are now presented together in a simple, unifying manner in which additional new T_m profiles are also included.

The T_m profiles obtained with mono- and dienoic PE shown diagonally in Fig. 3 can be explained by a MM-based molecular model proposed earlier from this laboratory [7,8]. The essence of this model is that the short segment in the kinked *sn*-2 acyl chain is largely disordered at $T < T_m$ and hence it acts principally as a perturbing element. The observed T_m-lowering effect of acyl chain monounsaturation can thus be accounted for quite simply by the presence of this perturbing element at $T < T_m$. In addition, according to the MM-based molecular model, the long segment in the kinked *sn*-2 acyl chain is assumed to be highly ordered at $T < T_m$; hence, unlike the short segment, it contributes significantly to the chain melting process at T_m. We can now apply the MM-based molecular model to the T_m profiles observed in those diagonal terms of Fig. 3. When the *cis* double bond(s) is located in the middle of the *sn*-2 acyl chain, the length of the long segment is minimal; thereby causing the lowest T_m. As the *cis* double bond(s) moves stepwise away from the chain middle toward either end, the length of the long segment increases progressively leading to a gradual increase in T_m.

This research was supported, in part, by U.S. Public Health Service Grant GM-17452 from NIGMS, National Institutes of Health, Department of Health and Human Services.

References

[1] D. Chapman, in: M. Shinitzkz (Ed.), Biomembranes: Physical Aspects, Balaban, Weinhein, 1993, pp. 29–63.
[2] Q. Ye, R.L. Biltonen, in: H.J. Hilderson, G.B. Ralston (Eds.), Subcellular Biochemistry, Vol. 23, Plenum Press, New York, 1994, pp. 121–160.
[3] T.E. Thompson, M.B. Sankaram, C. Huang, in: J.F. Hoffman, J.D. Jamieson (Eds.), Handbook of Physiology: Cell Physiology, Oxford University Press, New York, 1997, pp. 23–56.

[4] C. Huang, Z. Wang, H. Lin, E.E. Brumbaugh, S. Li, Biochim. Biophys. Acta 1189 (1994) 7–12.
[5] J.F. Nagle, R. Zhang, S. Tristram-Nagle, W. Sun, H.L. Petrache, R.M. Suter, Biophys. J. 70 (1996) 1419–1431.
[6] S. Li, H. Lin, Z. Wang, C. Huang, Biophys. J. 66 (1994) 2005–2018.
[7] Z. Wang, H. Lin, S. Li, C. Huang, J. Biol. Chem. 269 (1994) 23491–23499.
[8] C. Huang, H. Lin, S. Li, G. Wang, J. Biol. Chem. 272 (1997) 21917–21926.
[9] P. Comfurius, R.F.A. Zwall, Biochim. Biophys. Acta 488 (1977) 36–42.
[10] H. Xu, F.A. Stephenson, H. Lin, C. Huang, Biochim. Biophys. Acta 943 (1988) 63–75.
[11] H. Lin, Z. Wang, C. Huang, Biochemistry 29 (1990) 7063–7072.
[12] W.W. Christie, R.T. Holman, Chem. Phys. Lipids 1 (1967) 407–423.
[13] P.B. Hitchcock, R. Mason, K.M. Thomas, G.G. Shipley, Proc. Natl. Acad. Sci. USA 71 (1974) 3036–3040.
[14] S. Li, C. Huang, J. Comp. Chem. 17 (1996) 1013–1024.
[15] K.M.W. Keough, G. Griffin, N. Kariel, Biochim. Biophys. Acta 902 (1987) 1–10.
[16] M.P. Sanchez-Migallon, F.J. Aranda, J.C. Gomez-Fernandez, Biochim. Biophys. Acta 1279 (1996) 251–258.